The 2009 IEEE/RSJ International Conference on
Intelligent Robots and Systems
October 11-15, 2009 St. Louis, USA

An Electricity-Free Snake-Like Propulsion Mechanism Driven and Controlled by Fluids

Hisashi Date and Yoshihiro Takita

Abstract— **Unlike ordinary snake-like robots, a propulsion mechanism that does not rely on electricity for control and actuation is proposed in this paper. Analysis of a snake's propulsion based on a continuum model unveils that the lateral undulation can be achieved by bending the body at torque proportional to the curvature derivative of the body curve, as observed in muscular activities of biological snakes. Thanks to the simplicity of this principle, a pure mechanical structure comprising a fluid servomechanism can be realized. The proposed propulsion mechanism also consists of gears that propagate the joint angle information to the posterior joint to mechanically simulate curvature derivative.**

I. INTRODUCTION

Snake-like robots have been attracting growing interest, particularly as surgical instruments used for surveillance functions.These purposes may utilize the unique motion of snake, of which the most commonly seen gait is lateral undulation. The fundamentals are in lateral constraint, which is, transforming the bending motion into movement by preventing the side slip. On a rough terrain, it is easy to find some supporting objects such as rocks or plant. Snakes can progress by choosing appropriate supports and pushing on them [1]. On a flat terrain, however, some species of snakes make their scales on the belly ridged which behaves like the edge of a ski to prevent side slip [2]. This seems to be the result of evolution to overcome the shortcomings of the only available motion snakes have.

From the viewpoint of using a snake-like robot as a surveillance device on a rough terrain, while the mechanism is much different from that of snakes, the articulated crawler vehicle seems to actually be the most successful and efficient mechanism for propulsion at present [11], [12]. The crawler vehicle experiences inherent dimensional limitations due to the dead space for the return path of the belt. This prevents it from exploring a narrow spaces or tightly curved areas. A similar limitation lies in existing snake-like robots that use DC motors to drive joints. These includes having large spaces for high gear ratio to produce large torque and heavy weight due to the motors. Sinuous motion, however, still has an advantage once it acquires a smooth surface and has tiny lightweight actuators, as snakes in nature do. Therefore, alternative actuators might be a potential solution to these limitations.

While most existing snake-like robots are driven by DC motors or RC servos and controlled by micro computers, some are driven by pneumatic actuators with compressed air or hydraulic actuators with external pumps. Ohno et al have proposed a slime robot driven by pneumatic actuators. Each actuator is controlled by a built-in solenoid valve, which is controlled by one-chip microcomputers. In order to accommodate to a narrow space, inch worm like gait is chosen rather than lateral undulatory locomotion. This is necessary as long as the robot has to move by itself. When using a particular kind of endoscope, all we need is to assist the cord body to progress through complicated environments. Lateral undulatory locomotion will be suitable for such situation. Liljeback et al developed a fire fighting snake robot driven by water hydraulic actuators. Thanks to this kind of actuator, the joint can produce a torque as large as 311 Nm, which might help moving or prying disaster debris. Each actuator is controlled by a rotary valve driven by a DC servo motor. Both of the above examples still require electricity for control.

Mechanisms that use fluid as a means of control has quite a long history. One good example is a power steering system of an automobile [5]. It has a steering wheel as the input, and steered wheels are driven by hydraulic actuators. A valve opens when the desired angle is different from the actual wheel angle. Then hydraulic pressure drives the piston connected to the steered wheel until it comes to the right position where the actual wheel has the same angle as the steering wheel. Hence a negative feedback is organized in a mechanical manner. If a robot can be controlled by this kind of mechanism, it will benefit disaster environments especially when electric power fails

The authors have proposed a continuum model for lateral undulatory locomotion under the assumption that there is no slip in lateral direction [6]. Mathematical analysis has revealed that a joint torque proportional to the curvature derivative is optimal for reducing total power lost during progression. This result agrees to muscular activities in living snakes [7]. The continuum model can be easily approximated to a finite rigid link model by approximating the curvature derivative using the difference of adjacent joint angles. The result is a simple proportional control where the anterior joint angle is the reference angle of the posterior joint. This simplicity contributes to implementation in various ways. This scheme has been verified by DC-motor powered prototypes in various environments including flat terrains, smoothly curved surfaces, or a single peg [6], [8].

In this paper, a new fluid controlled and driven mechanism based on the continuum model is proposed. Combining the simplicity of the approximated optimal control and the traditional fluid servomechanism, it utilizes links length of 16mm,

H. Date and Y. Takita are with Department of Computer Science, National Defense Academy, 1-10-20 Hashirimizu, Yokosuka, Kanagawa, Japan {date, takita}@nda.ac.jp

a width of 38 mm, and a minimum curvature radius of 60mm. It no longer has control circuit boards. Instead, it consists of high pressure lines for fluid and gearing mechanism that propagate the joint angle information to the posterior joints. Actuators are replaced by a pair of simple pistons.

II. CONTINUUM MODEL

The continuum model under the assumption that there is no lateral slippage and its approximation for rigid link model is briefly reviewed in this section.

The continuum model consists of a smooth curve of zero thickness parameterized by its arc length $s \in [0, L]$. On each point $O(s)$ of the curve, a frame set consisting of three orthonormal bases e_1, e_2, e_3 is attached, where e_1 corresponds to the tangent of the curve O'. Hereafter, derivative with respect to arc length s is denoted by by the prime sign $(')$, time derivative by over dot $(\dot{})$, and inner product of two vectors by $\langle \cdot, \cdot \rangle$. Here we assume the following conditions.

1) The backbone is not stretchable ($\|e_1\| = const.$)
2) The backbone is torsion free ($\langle e_2', e_2 \rangle = \langle e_3', e_2 \rangle = 0$)
3) Lateral velocity is zero
$$\langle \dot{O}, e_1 \rangle = -v, \langle \dot{O}, e_2 \rangle = \langle \dot{O}, e_3 \rangle = 0$$
where v is the progress speed along $-e_1$
4) There is no longitudinal friction
5) Rotation around the curve is not restricted except for the head
6) Bending moment τ_2, τ_3 respectively along e_2, e_3 defined as
$$\kappa_i = \langle O', e_i \rangle \quad (i = 2, 3)$$
can be generated at arbitrary point of the body

The motion of equation of the entire system can be given by

$$m\alpha = -\int_0^L (\kappa_2' \tau_3 - \kappa_3' \tau_2)\, ds \tag{1}$$

where α is the forward longitudinal acceleration and κ_2, κ_3 are the curvatures around e_2, e_3, respectively.

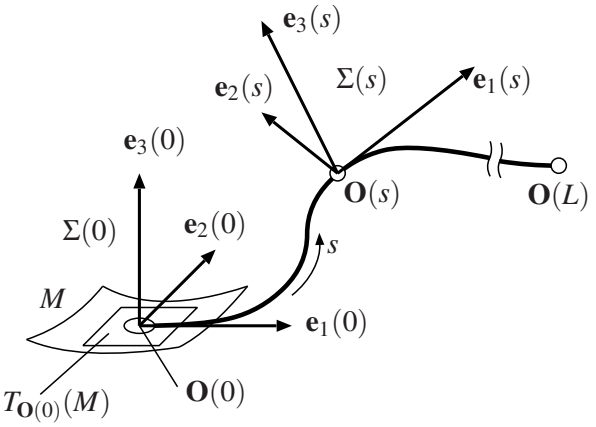

Fig. 1. Continuum model consisting of smooth backbone curve with zero thickness moving forward with acceleration α

The optimal bending moment that minimizes the quadratic cost function

$$J = \int_0^L \left(\tau_2^2 + \tau_3^2\right) ds$$

can be derived by solving isoperimetric problem [6] as follows:

$$\begin{bmatrix} \tau_2 \\ \tau_3 \end{bmatrix} = -\frac{m\alpha}{\int_0^L (\kappa_2'^2 + \kappa_3'^2) ds} \begin{bmatrix} -\kappa_3' \\ \kappa_2' \end{bmatrix} \tag{2}$$

This continuum model can be approximated to a rigid link model by the following assignments: Curvature $(\kappa_2(s), \kappa_3(s)) \rightarrow i$th joint angle $(\phi_2[i], \phi_3[i])$; bending moment $(\tau_2(s), \tau_3(s)) \rightarrow$ joint torque $(\tau_2[i], \tau_3[i])$ on ith joint. Thus we have

$$\begin{bmatrix} \tau_2[i] \\ \tau_3[i] \end{bmatrix} = K(v_d - v) \begin{bmatrix} \phi_2[i-1] - \phi_2[i] \\ \phi_3[i-1] - \phi_3[i] \end{bmatrix} \tag{3}$$

as the discrete approximation, where K is the control gain that governs the longitudinal acceleration and v_d is the desired longitudinal velocity. (3) simply forms P control of the posterior joints $(\phi_2[i], \phi_3[i])$ whose references are the anterior joint angles $(\phi_2[i-1], \phi_3[i-1])$.

In the two dimensional case, joint angle and torque vectors are simply substituted by scalar values $\phi[i]$ and $\tau[i]$, respectively, as follows.

$$\tau[i] = K(v_d - v)(\phi[i-1] - \phi[i]) \tag{4}$$

III. APPLICATION TO ENDOSCOPE

Passive endoscopes should be thin and flexible in order to reach a deep parts of the subject. However, too much flexibility prevents the scope from passing through curve section, particularly at turning points. Buckling may occur even in a straight section. Therefore commercial endoscopes should have moderate stiffness to maintain adequate manipulability. Some active endoscopes that utilize Shape Memory Alloy (SMA) to make the tip maneuverable for arbitrary direction [9], [10]. There is a statement concerning reduction of stress on the tissue of the patient's body by using active bending mechanism at every part of the body. Snake-like lateral undulatory locomotion does this in an efficient manner as described below.

Fig.2 draws a scene where the active endoscope is inserted into a subject with a somewhat complicated ventricle. The entrance section is not curved a lot, so there is no great stress on the wall. In this case, the lateral undulatory mechanism cannot produce propulsion because of the singular posture. On the contrary, at the first right turn, purely passive endoscopes might be jammed, and further progress will become harder while non-zero curvature derivative allows the snake-like mechanism to produce propulsion as well as reducing the stress on the wall. In this sense, lateral undulatory locomotion is a good complement of the endoscope.

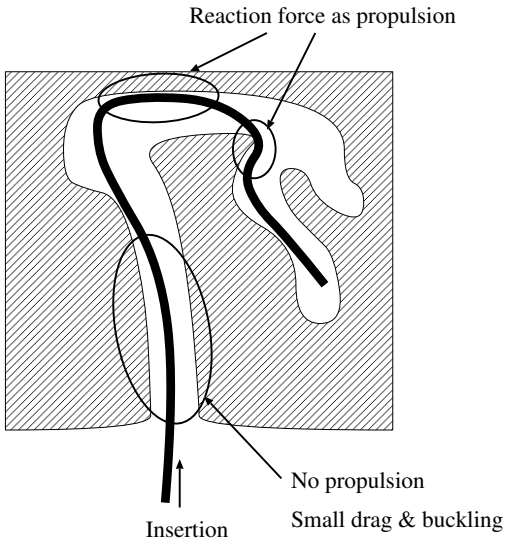

Fig. 2. Snake-like mechanism as an endoscope; Lateral undulation does not function during less curved section. It produces propulsion at corners where a passive device might fail to progress due to buckling

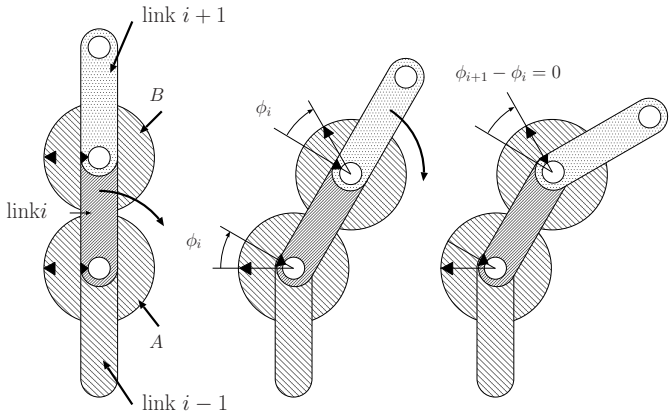

Fig. 3. Propagation of joint angle: Difference in two joint angles $\phi_{i+1} - \phi_i$ appears in the relative angle of gear B to $i+1$th link

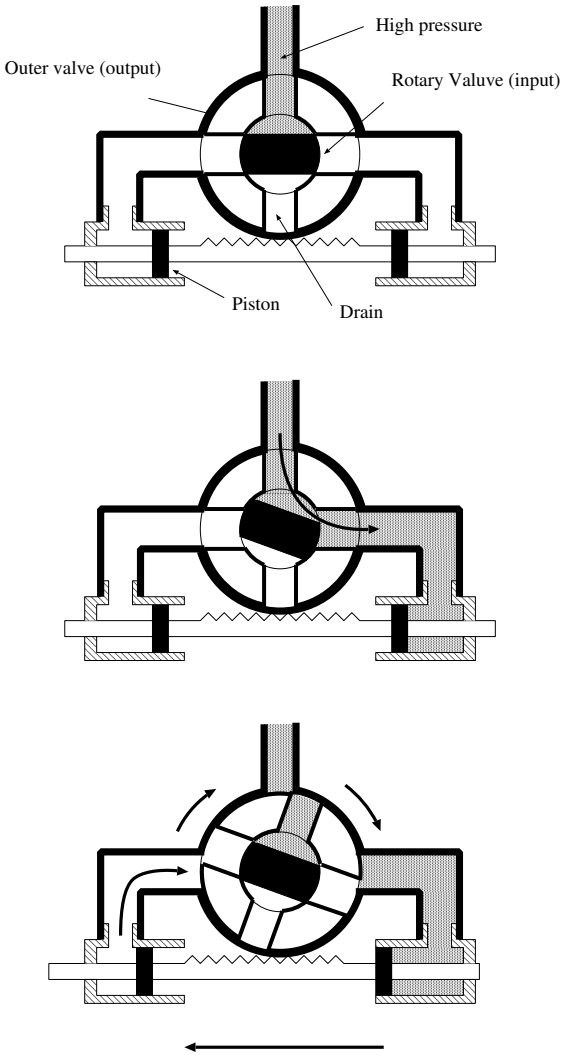

Fig. 4. Schematic diagram of automotive power steering system: Outer valve is geared with the lack connected to the hydraulic piston. The outer valve closes when it has the same angle as the input rotary valve.

IV. PROPULSION MECHANISM USING FLUID

The proposed mechanism consists of mainly two components. One is the transfer mechanism of joint angle. In order to simulate curvature derivative, adjacent joints must share the joint angle information. The other is fluid servomechanism.

A. Simulating Curvature Derivative

Curvature derivative is approximated by the difference in joint angles of the posterior joint and anterior joint as expressed in (4). The following are important in mechanical implementation:

- Zero error must be realized by mechanical agreement
- Rotational difference must be realized on a common axis

Fig. 3 shows how the above requirements can be realized using a pair of identical gears. Mechanical elements painted with the same pattern denotes mutually fixed or geared elements. Three independent groups of elements are drawn. The gear A is attached to the link $i-1$ and geared to the gear B. An arrow mark is drawn on each gear and link to indicate their original position. From the left figure to the middle, the $i-1$th joint is bent clockwise at angle ϕ_i. Then the gear B turns $2\phi_i$ clockwise. So the relative angle between $i+1$th link and the gear B is identical to ϕ_i. In the right figure, the $i+1$th link is bent at the same angle ϕ_i clockwise relative to the ith link, where both arrow marks are congruent. Hence, the difference of joint angle $\phi_{i+1} - \phi_i$ can be formed as the angle between the two arrow marks.

B. Fluid Servomechanism

Conventional hydraulic power steering system for automotive can be regarded as a servomechanism where the steering wheel angle is the reference angle and the actual

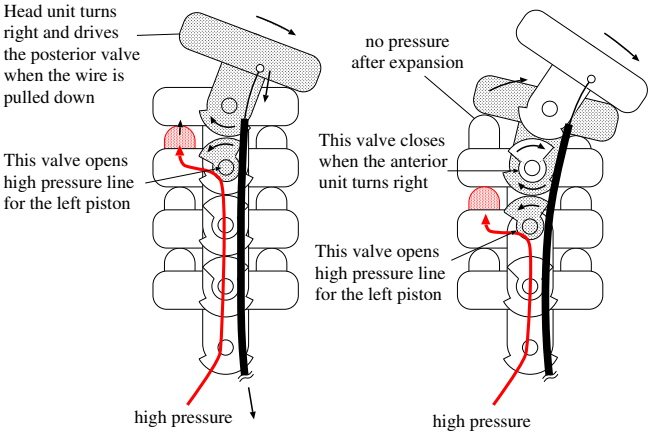

Fig. 5. Schematic drawing of the first unit motion: When the head unit turns right pulled by the wire, the next input valve turns reversely and the left piston will be pressurized. Once the 2nd joint has the angle same as the first, high pressure is no longer applied to the first left piston

wheel angle is the output. Valve mechanism is linked to the feedback error, namely, the difference between the input and output. Thus hydraulic power is supplied to attenuate the error as long as the valve is open. Fig. 4 shows the basic action of a standard power steering system. The size of valve orifice depends on the relative position of the rotary and outer valves. Thus the steering angle can be stabilized at arbitrary angle.

C. Integration

Fluid servomechanism must have three independent elements; input, output, and base. These three elements should be constructed on each joint. On the ith joint, the input is connected to the gear B. The output is connected to the $i+1$th link. The base in this case is the ith link. The actuator is located between ith link and $i+1$th link to produce torque between these elements. The valve system is organized to be dependent on the relative position of the input and output. When there is a difference in angle between the gear B and $i+1$th link, a gap appears in the valve to drive the actuator so that the gap becomes smaller.

The first unit determines the direction of progress because the posterior units follow the same joint angles afterwords. The operator manipulates this part like a steering of a vehicle via wire or other remote control methods as shown in Fig. 5. If there exists a wall that can guide the head unit, the guide rollers will suffice for exploration.

V. PROTOTYPE

A. Mechanism

Fig. 6 shows the front view of the prototype. The maximum bending angle of each joint is about 14 degrees. The center distance of each joint is 16 (mm), so the minimal inner radius is approximately 100 (mm). The head unit has guide rollers on the both sides, so no wire is installed to manipulate it. The materials consists of aluminum alloy

Fig. 6. Front view of partly assembled prototype; 15 units are joined. The first two units are used as a "steering", so no air pressure is supplied.

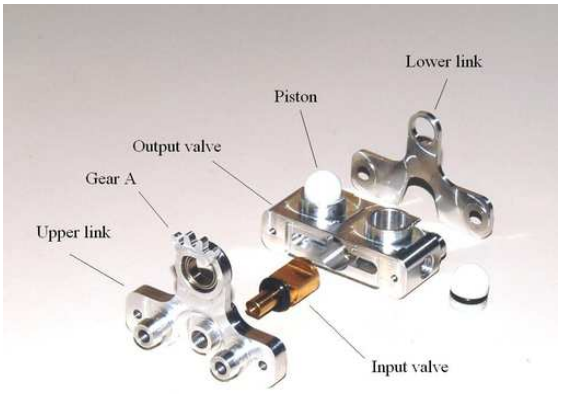

Fig. 7. Disassembled unit

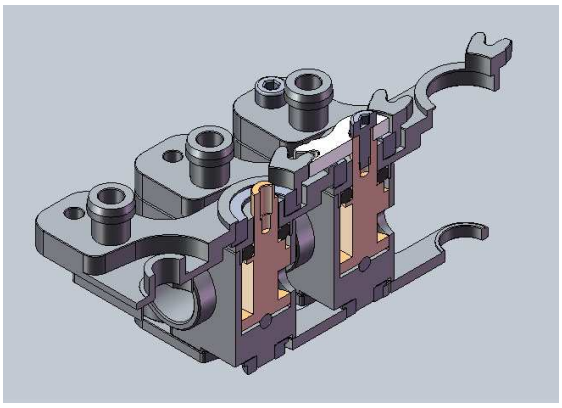

Fig. 8. Cross section of minimal configuration

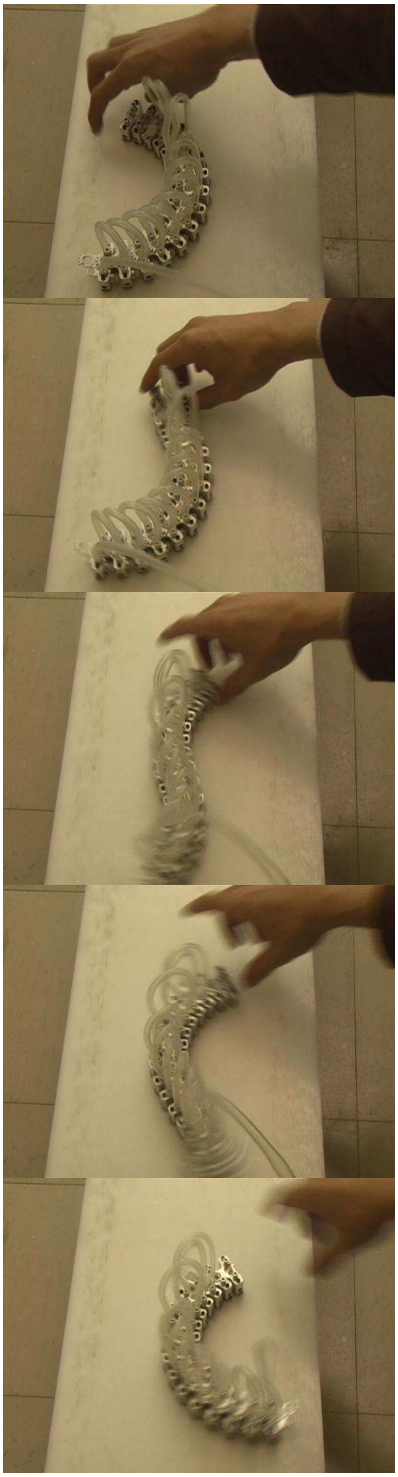

Fig. 9. Motion without lateral constraints: The head unit is manually turned right and the body rapidly change its shape from mirrored C-shape to C-shape

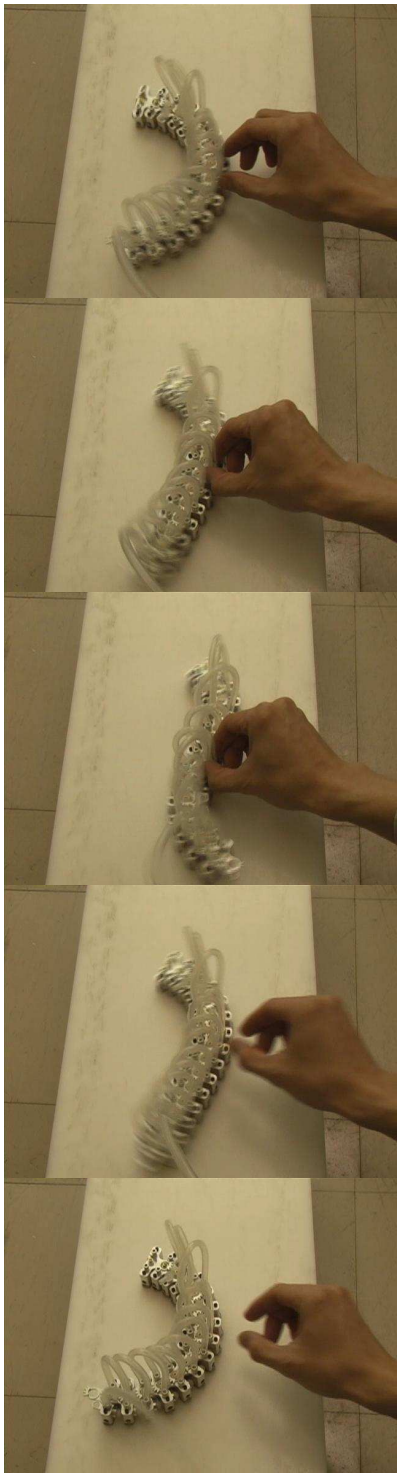

Fig. 10. External torque applied on an intermediate joint. While there is no effect on antecedent joint, the curve is reversed in the downward section. It rapidly recovers once hand is released.

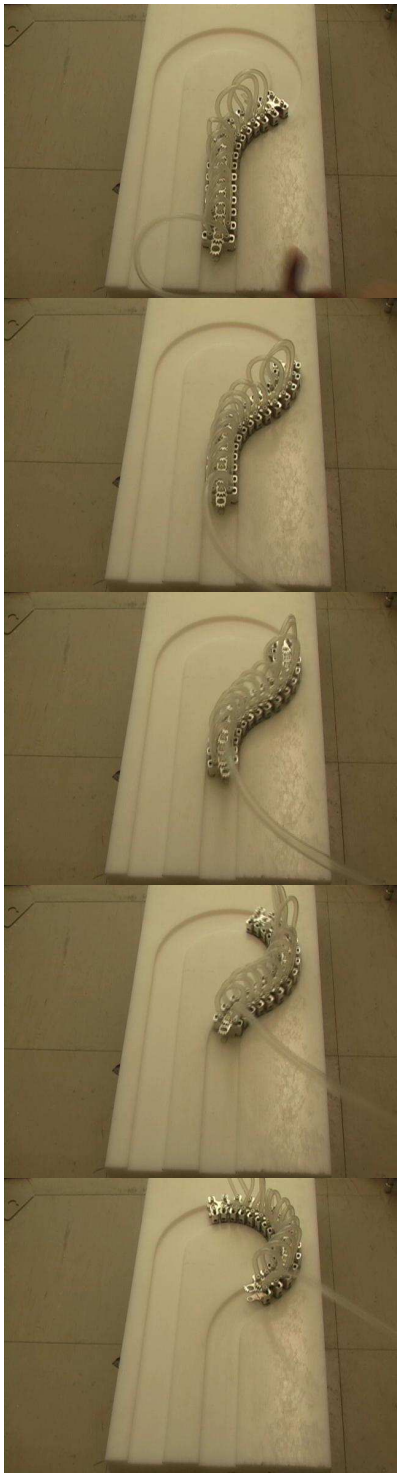

Fig. 11. Progress along a groove consisting of straight lines and arcs. Propulsion is no longer generated in the circular section where the curvature derivative is uniformly zero.

TABLE I

BRIEF SPECIFICATION OF COMPONENTS

Component	Material	Dimension (mm)
Input valve	Brass	ϕ 8
Output valve	Duralumin	40×10×18
Upper / Lower link	Duralumin	Cent. dist. 16
Gear A	(part of the upper link)	Pitch dia. 16
Gear B	Polyacetal	Pitch dia. 16
Piston	Polyacetal	ϕ 8

(duralumin), brass, and polyacetal. The disassembled components are shown in Fig. 7. All parts are machined using CNC. Gear cogs are not fully made to avoid interference between coaxially located gears A and B. High pressure air is supplied from the last unit, i.e., the tail, and the line is succeeded via silicone flexible tube to the antecedent units. Each unit weighs 31.5 (g) including tubes. Table I summarizes brief specifications of the components. Each joint produces a torque up to 0.042 (Nm) under 0.1 (MPa) of pressure supply. Although air is used in the following cases, liquids including water or oil are available as long as the fluid servomechanism works.

B. Experiments on a flat surface

The prototype is first tested on a flat surface to ensure the basic functionality – whether the anterior joint angles are propagated to the posterior joint.

Since there are no lateral constraints, it behaves like a "live caught fish" and the shape of the body eventually converges to a constant curvature shape, namely a straight line or an arc (Fig.9). Note that many literatures on lateral undulatory locomotion by a robot deals with winding gait as "shape change" and hence explicit wave propagation is implemented by controlling joint angles with a certain constant phase shift. In that scheme, the body cannot adapt to disturbances away from the scheduled gait.

Fig. 10 shows the case when an external torque is applied on an intermediate joint. This implies capability of adaptation to an unpredictable environment change. Borrowing the words from "mobiligence" [13], this mechanism has *embodied plasticity*.

C. Propulsion along a Winding Curve

A testbed made of polyacetal block is used to test propulsion. A groove of depth 6 (mm) and width 41 (mm) is carved on the surface as a guide consisting of straight track and three quarters of a circle of diameter 120 (mm). Thanks to the lateral constraint by the groove's wall, the body begins to move once air pressure is supplied unlike the case on a flat surface (Fig. 11). It stops in the midst of a circular track where the curvature is constant. Note that using circular path is not very good idea for winding path according to the mathematical model because circular part has constant curvature except for the inflection points. This means that the curvature derivative is zero everywhere other than the inflection point. Therefore only one or two joints are actually active resulting small propulsion and high resistance. The situation may be improved if the groove is a bit more wider than the body width. In this case, some units may have no contact with the wall and the resultant body shape will have smoother curvature change even in circular S-shape. Effectiveness of curvature derivative control in a wider winding corridor has been proved using a prototype equipped with DC-motors [8]. The corresponding video file is attached to this manuscript for Fig. 9, 10 and 11.

VI. CONCLUSION

In this paper, fluid powered and controlled snake-like propulsive mechanism is presented. It should be emphasized that lateral undulatory locomotion does not necessarily requires explicit propagation of body shape such as phase shift. Instead, mechanically implementable structure derived from the continuum model has turned out to possess adaptability and capability of progressing once an appropriate environment is supplied. Hence electricity free control system is achievable. This point is quite insightful from the perspective of a new "mobiligence" approach.

This paper presented only several pieces of motion of the mechanism. For quantitative discussion, further experiments should be conducted.

REFERENCES

[1] J. Gray and H. W. Lissmann, The kinetics of locomotion of the grass-snake, Experimental Biology, Vol. 26, pp. 354-367, 1950

[2] S. Hirose, Biologically Inspired Robots: Snake-like Locomotors and Manipulators, Oxford University Press, 1993

[3] H. Ohno and S Hirose. Study on slime robot (proposal of slime robot and design of slim slime robot), In Proc. of the IEEE/RSJ International Conference on Intelligent Robots and Systems, pp 2218-2223, 2000.

[4] P. Liljeback, O. Stavdahl, and A. Beitnes, Snake-fighter -development of a water hydraulic firefighting snake robot, In Proc. Intl. Conf. Control, Automation, Robotics and Vibration, pp. 1-6, 2006.

[5] F. W. Davis, Hydraulic Steering Mechanism, U.S. Patent #1,790,620, 1931

[6] H. Date and Y. Takita, Control of 3D Snake-like locomotive mechanism based on continuum modeling, In Proc. ASME Intl. Design Eng. Tech. Conf. & Comp. Info. in Eng. Conf. (IDETC), No. DETC2005-85130, 2005

[7] B.R. Moon and C. Gans, Kinematics, Muscular Activity and Propulsion in Gopher Snake, In Journal of Experimental Biology, Vol. 201, pp. 2669–2684, 1998

[8] H. Date, Y. Takita, Adaptive Locomotion of a Snake Like Robot Based on Curvature Derivatives, In Proc. of the IEEE/RSJ International Conference on Intelligent Robots and Systems, pp 3554-3559, 2007.

[9] G. Lim, et al., Future of active catheters, Sensors and Actuators, A56, pp. 113-121(1996)

[10] Y. Koseki, N. Koyachi, T. Arai, Development of spiral structure for active catheter: Overview of spiral structure and its kinematic configurations, In Proc. of the IEEE/RSJ International Conference on Intelligent Robots and Systems, Vol. 2, pp. 1259-1264, 1999

[11] K. Osuka and H. Kitajima, Development of Mobile Inspection Robot for Rescue Activities: MOIRA, In Proc. of the IEEE/RSJ International Conference on Intelligent Robots and Systems, pp 3373–3377, 2003.

[12] M. Arai, T. Takayama, S. Hirose, Development of "Soryu-III": Connected Crawler Vehicle for Inspection inside Narrow and Winding Spaces, In Proc. of the IEEE/RSJ International Conference on Intelligent Robots and Systems, pp 52–57, 2004.

[13] H. Asama, M. Yano, K. Tsuchiya, K. Ito, H. Yuasa, J. Ota, A. Ishiguro, T. Kondo, System Principle on Emergence of Mobiligence and Its Engineering Realization, In Proc. of the IEEE/RSJ International Conference on Intelligent Robots and Systems, pp 1715–1720, 2003.